

# Quantum Transport with Spin Dephasing: A Nonequilibrium Green's Function Approach

Ahmet Ali Yanik\*

*Department of Physics, and  
Network for Computational Nanotechnology,  
Purdue University, West Lafayette, IN, 47907, USA*

Gerhard Klimeck

*School of Electrical and Computer Engineering,  
Network for Computational Nanotechnology,  
Purdue University, West Lafayette, IN, 47907, USA and  
Jet Propulsion Lab, Caltech, Pasadena, CA, 91109, USA*

Supriyo Datta

*School of Electrical and Computer Engineering and  
Network for Computational Nanotechnology,  
Purdue University, West Lafayette, IN, 47907, USA*  
(Dated: January 26, 2020)

A quantum transport model incorporating spin scattering processes is presented using the non-equilibrium Green's function (NEGF) formalism within the self-consistent Born approximation. This model offers a unified approach by capturing the spin-flip scattering and the quantum effects simultaneously. A numerical implementation of the model is illustrated for magnetic tunnel junction devices with embedded magnetic impurity layers. The results are compared with experimental data, revealing the underlying physics of the coherent and incoherent transport regimes. It's shown that spin scattering processes are suppressed with increasing barrier heights while small variations in magnetic impurity spin-states/concentrations could cause large deviations in junction magnetoresistances.

PACS numbers: 72.10.-d, 72.25.-b, 72.25.Rb, 71.70.Gm, 73.43.Qt

## I. INTRODUCTION

Quantum transport in spintronic devices is a topic of great current interest. Most of the theoretical work reported so far has been based on the Landauer approach [1] assuming coherent transport, although a few authors have included incoherent processes through averaging over a large ensemble of disordered configurations [2, 3, 4]. However, it is not straightforward to include dissipative interactions in such approaches. The non-equilibrium Green's function (NEGF) formalism provides a natural framework for describing quantum transport in the presence of incoherent and even dissipative processes. Here, a numerical implementation of the NEGF formalism with spin-flip scattering is presented. For magnetic tunnel junctions (MTJs) with embedded magnetic impurity layers, this model is able to capture and explain three distinctive experimental features reported in the literature [5, 6, 7, 8] regarding the dependence of the junction magnetoresistances (*JMRs*) on (1) barrier thickness, (2) barrier height and (3) the number of magnetic impurities. The model is quite general and can be used to analyse and design a variety of spintronic devices beyond the 1-D

geometry explored in this article.

This article is organized as follows. In the view of pedagogical clarity, a heuristic presentation of the NEGF formalism with spin dephasing mechanisms is given Sec II followed by a numerical implementation of the model in Sec III. Initially (Sec III A) the definitions of device characteristics are presented for *impurity free* MTJs together with device parameters benchmarked against experimental measurements. How to incorporate the spin exchange scattering mechanisms into the electron transport calculations are shown (Sec III B), and the model is applied to MTJ devices with magnetic impurity layers (Sec III C). Theoretical estimates and experimental measurements are compared as well in this section (Sec III C), while a summary of the results is given in Sec IV.

## II. MODEL DESCRIPTION

*NEGF Method:* The problem is partitioned into channel and contact regions as illustrated in Fig. 1 [9]. Inputs can be classified in four categories:

- (i) *Channel* properties are defined by the Hamiltonian matrix [ $H$ ] including the applied bias potential.
- (ii) *Contacts* are included through self-energy matrices

---

\*Electronic address: yanik@purdue.edu

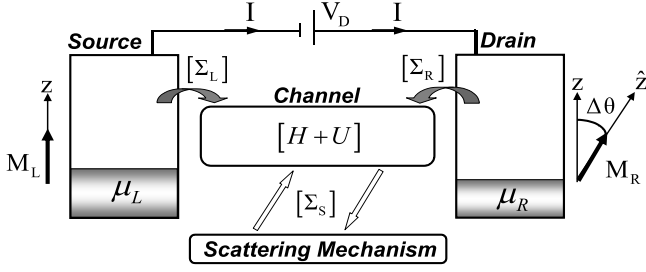


FIG. 1: Schematic illustration of the NEGF inputs needed for quantum transport calculations. Magnetization direction of the drain is defined relative to the source ( $\Delta\theta = \theta_R - \theta_L$ ).

$[\Sigma_L]/[\Sigma_R]$  whose anti-hermitian component

$$\Gamma_{L,R}(E) = i \left( \Sigma_{L,R}(E) - \Sigma_{L,R}^\dagger(E) \right) \quad (1)$$

describes the broadening due to the coupling to the contact. The corresponding inscattering/outscattering matrices are defined as:

$$\Sigma_{L,R}^{in}(E) = f_0(E - \mu_{L,R}) \Gamma_{L,R}(E), \quad (2a)$$

$$\Sigma_{L,R}^{out}(E) = [1 - f_0(E - \mu_{L,R})] \Gamma_{L,R}(E), \quad (2b)$$

where  $f_0(E - \mu_{L,R}) = 1/1 + \exp[(E - \mu_{L,R})/k_B T]$  is the Fermi function for the related contact.

(iii) *Electron-electron interactions* are incorporated through the self-consistent potential matrix  $[U]$ .

(iv) *Incoherent* scattering processes in the channel region are described by in/out-scattering matrices

$$\Sigma_{S,\sigma_i,\sigma_j}^{in}(r,r';E) = \int \sum_{\sigma_k,\sigma_l} D_{\sigma_i\sigma_j;\sigma_k\sigma_l}^{n,p}(r,r';\hbar\omega) G_{\sigma_k\sigma_l}^n(r,r';E - \hbar\omega) d(\hbar\omega). \quad (8)$$

where  $[D^n]/[D^p]$  are fourth-order tensors, describing the spatial correlation and energy spectrum of the underlying microscopic *spin-conserving/spin-randomizing* scattering mechanisms. The indices  $(\sigma_k, \sigma_l)/(\sigma_i, \sigma_j)$  are used to refer the *initial/final* spin components.

*Current* is calculated from the self-consistent solution of the above equations for any terminal "i";

$$I_i = \frac{q}{h} \int_{-\infty}^{\infty} \text{trace} \left( [\Sigma_i^{in}(E) A(E)] - [\Gamma_i(E) G^n(E)] \right) dE. \quad (9)$$

Solution scheme without going into the details could be summarized as follows. The inputs listed under the categories (i) and (ii) are fixed at the outset of any calculations. Whereas the inputs  $[U]$ ,  $[\Sigma_S^{in,out}]$  and  $[\Sigma_S]$  under

$[\Sigma_S^{in}]/[\Sigma_S^{out}]$ . Broadening due to scattering is given by;

$$\Gamma_S(E) = [\Sigma_S^{in}(E) + \Sigma_S^{out}(E)], \quad (3)$$

from which the self-energy matrix is obtained through a Hilbert transform:

$$\Sigma_S(E) = \frac{1}{2\pi} \int \frac{\overbrace{\Gamma_S(E')}^{\text{Re}}}{E' - E} dE' - i \frac{\overbrace{\Gamma_S(E)}^{\text{Im}}}{2}. \quad (4)$$

Eqs. (1-2) are the boundary conditions that drive the coupled NEGF equations [Eqs. (3-8)], where Green's function is defined as;

$$G = [EI - H - U - \Sigma_L - \Sigma_R - \Sigma_S]^{-1}, \quad (5)$$

with the spectral function (analogous to density states);

$$A = i [G - G^+] = G^n + G^p. \quad (6)$$

where  $[G^n]/[G^p]$  refer the *electron/hole correlation functions* (whose diagonal elements are the electron/hole density):

$$G^{n,p} = G \left[ \Sigma_L^{in,out} + \Sigma_R^{in,out} + \Sigma_S^{in,out} \right] G^+. \quad (7)$$

The in/out-scattering matrices  $[\Sigma_S^{in}]/[\Sigma_S^{out}]$  are related to the electron/hole correlation functions  $[G^n]/[G^p]$  by;

the *charging and scattering* categories (iii) and (iv) depend on the correlation and spectral functions requiring an *iterative self-consistent solution* of the NEGF Equations [Eqs. (3-8)]. One important thing to note is that in the following numerical implementation of the NEGF model charging potential matrix  $[U]$  is left out of the discussion due to the tunneling nature of the transport. This allows one to focus on the *dephasing* due to the spin-flip interactions.

### III. APPLICATION: MTJs WITH MAGNETIC IMPURITIES

Electron transport is considered *coherent* by standard definitions if through the course of electron's journey

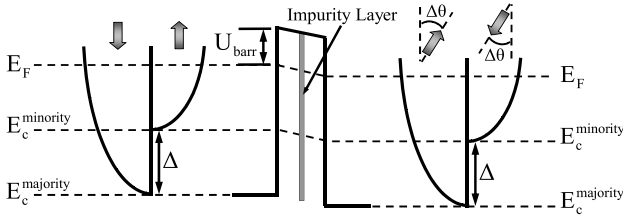


FIG. 2: Energy band diagram for the model MTJs.

from source to drain state of nothing else changes. Accordingly scatterings from "rigid" impurities are considered as coherent processes whereas incoherent processes are mainly viewed as inelastic meaning they involve energy exchange between the electron and the impurities through which impurities are set into a jiggling motion. Yet it's not necessary that every incoherent process involves an exchange of energy between the electron and the impurity. A good example to this will be investigated in this part of the paper for electron-impurity spin exchange scattering processes in MTJs.

### A. MTJs in Coherent Regime

In this section, MTJ device fundamentals and the tunneling transport characteristics are presented in the absence of magnetic impurities (*the coherent regime*). MTJs consisting of a tunneling barriers ( $\text{AlO}_x$ ) sandwiched between two ferromagnets (Co) with different magnetic coercivities enabling independent manipulation of their magnetization directions (Fig. 2) is considered here. Single band free electron theory with a constant bare electron mass ( $m^* = m_e$ ) is used [10]. Under these conditions, transverse modes can be included using 2-D integrated Fermi functions  $f_{2D}(E_z - \mu_{L,R}) = (m^* k_B T / 2\pi \hbar^2) \ln [1 + \exp(\mu_{L,R} - E_z / k_B T)]$  in Eq. (2). Ignoring spin-orbit coupling, the device Hamiltonian is;

$$H = \begin{bmatrix} \alpha_1 & \beta & \cdots & \bar{0} & \bar{0} \\ \beta^+ & \alpha_2 & \cdots & \bar{0} & \bar{0} \\ \vdots & \vdots & \ddots & \vdots & \vdots \\ \bar{0} & \bar{0} & \cdots & \alpha_{N-1} & \beta \\ \bar{0} & \bar{0} & \cdots & \beta^+ & \alpha_N \end{bmatrix}. \quad (10)$$

with 2x2 on-site  $\alpha$  and site-coupling  $\beta$  matrices

$$\alpha_n = \begin{bmatrix} \alpha_n^\uparrow & 0 \\ 0 & \alpha_n^\downarrow \end{bmatrix} \quad \& \quad \beta = \begin{bmatrix} \beta_n^\uparrow & 0 \\ 0 & \beta_n^\downarrow \end{bmatrix}. \quad (11)$$

where  $\alpha_n^{\uparrow,\downarrow} = E_{c,n}^{\uparrow,\downarrow} + 2t + U_n$  and  $\beta_n^{\uparrow,\downarrow} = -t$  with  $t = \hbar^2 / 2ma^2$ . The self-energy matrix for the left/right contact is nonzero only first block for which we can write

$$\Sigma_L(1, 1, E_z) = \begin{bmatrix} -te^{ik_L^\uparrow a} & 0 \\ 0 & -te^{ik_L^\downarrow a} \end{bmatrix}, \quad (12)$$

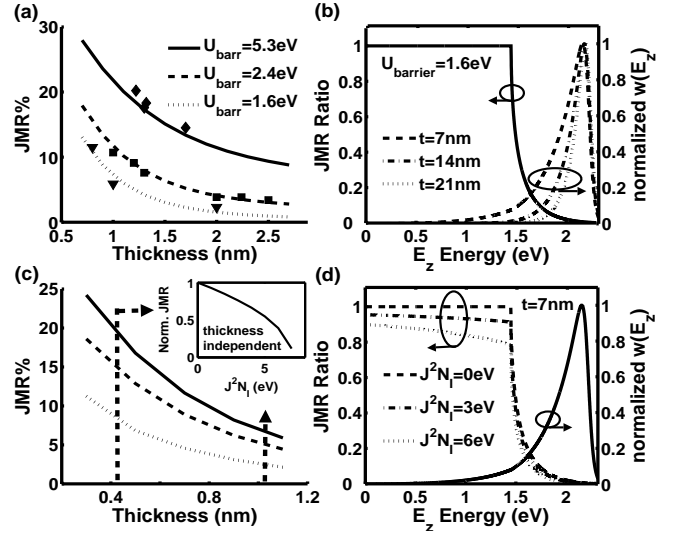


FIG. 3: For impurity free MTJs, (a) thickness dependence of *JMRs* for different barrier heights is shown in comparison with experimental measurements [11, 12, 13, 14, 15, 16, 17, 18, 19, 20], (b) energy resolved *JMR* ( $E_z$ ) (*left-axis*) and *normalized w* ( $E_z$ ) (*right-axis*) are also given for a device with a barrier height of 1.6 eV. For MTJs with impurity layers, (c) variation of *JMRs* for varying barrier thicknesses and interactions strengths are shown together with (d) a detailed energy resolved analysis. Normalized *JMRs* are proven to be thickness independent as displayed in the inset.

where  $E_z = E_c^{\uparrow,\downarrow} + U_L + 2t(1 - \cos k_L^{\uparrow,\downarrow} a)$ . For the right contact only the last block is non-zero;

$$\Sigma_R(N, N, E_z) = \bar{U}^+ \begin{bmatrix} -te^{ik_L^\uparrow a} & 0 \\ 0 & -te^{ik_L^\downarrow a} \end{bmatrix} \bar{U}, \quad (13)$$

where  $\bar{U}$  is the unitary transformation needed to rotate from the spin "up" and "down" directions of right contact ( $\theta_R, \phi_R$ ) into that of the left contact ( $\theta_L = 0, \phi_L = 0$ );

$$\bar{U}(\theta, \phi) = \begin{bmatrix} \cos(\theta/2) e^{i\phi/2} & \sin(\theta/2) e^{-i\phi/2} \\ -\sin(\theta/2) e^{i\phi/2} & \cos(\theta/2) e^{-i\phi/2} \end{bmatrix}. \quad (14)$$

*Theoretical analysis* of MTJ devices in the absence of magnetic impurity layers are presented and compared with the experimental data [5, 7] for varying tunneling barrier heights and thicknesses. The parameters used here for the generic ferromagnetic contacts are the Fermi energy  $E_F = 2.2$  eV and the exchange field  $\Delta = 1.45$  eV [10]. The tunneling region potential barrier [ $U_{barr}$ ] is parameterized within the band gaps quoted in literature [21, 22], while the charging potential [ $U$ ] is neglected due to the pure tunneling nature of the transport. Referring  $I_F / I_{AF}$  as the current values for the parallel/antiparallel magnetizations ( $\Delta\theta = 0 / \Delta\theta = \pi$ ) of the ferromagnetic contacts, *JMR* is given as;

$$JMR = \frac{I_F - I_{AF}}{I_F} = \int \omega(E_z) JMR(E_z) dE_z \quad (15)$$

where  $\omega(E_z) = I_F(E_z)/I_F$  is the energy resolved spin-continuum current component while  $JMR(E_z) = (I_F(E_z) - I_{AF}(E_z))/I_F(E_z)$  is defined as the *energy resolved junction magnetoresistance*.

*Coherent* tunneling regime features are obtained by benchmarking the experimental measurements made in impurity free tunneling oxide MTJs at small bias voltages. The dependence of the *JMRs* on the thickness and the height of the tunneling barriers is shown in Fig. 3(a) with an energy resolved analysis [Fig. 3(b)] for different barrier thicknesses (0.7 – 1.4 – 2.1 nm). *JMR* values are shown to be improving with increasing barrier heights for all barrier thicknesses, a theoretically predicted [7, 8] and experimentally observed [11, 12, 13, 14, 15, 16, 17, 18, 19, 20] feature in MTJs, although the barrier heights obtained here may differ from those reported in literature [11, 12, 13, 14, 15, 16, 17, 18, 19, 20] based on empirical models [23].

Decaying *JMRs* with increasing barrier thicknesses are observed [Fig. 3(a)], even though the energy resolved *JMR*( $E_z$ ) ratios are thickness independent [Fig. 3(b)]. This *counterintuitive* observation can be understood by considering the redistribution of tunneling electron densities over energies with changing tunneling barrier thicknesses. Here  $w(E_z)$  is the quantity defining the distribution of the tunneling electron densities. In Eq. (15) *JMR*( $E_z$ ) ratios are *constant* independently from the barrier thicknesses (solid line in Fig. 3(b)). while the *normalized*  $w(E_z)$  distributions shifts towards higher energies with increasing barrier thicknesses (dashed lines in Fig. 3(b)). Hence *JMRs*, an integral of the multiplication of  $w(E_z)$  distributions with the energy resolved *JMR*( $E_z$ ), decays with increasing barrier thicknesses (Eq. (15)).

## B. Adding Spin Exchange Scattering

Spin exchange scattering processes are responsible from the incoherent nature of the tunneling transport for the model devices considered here. Through this elastic scattering process, the state of nothing else seem to change if the electron and the impurity spins are considered as a composite system. Nevertheless, it is an incoherent process since the state of the impurity has

changed. Then what really makes this processes incoherent is the external forces forcing the impurity spins into local equilibrium. The incoherent nature of the scattering lies in the "information erasure" nature of the surrounding through the forces forcing the impurity spins into an unpolarized (%50 up, %50 down) spin distribution. These external forces such as in a closely packed impurity layer could be magnetic dipole-dipole interactions among the magnetic impurities or spin relaxation processes coupled with phononic excitations. Nevertheless the physical origin of the equilibrium restoring processes is not of our interest (at least from tunneling electron's point of view) assuming equilibrium restoring processes are fast enough to maintain the impurity spins in a thermal equilibrium state. Accordingly, dephasing effect of the surrounding could be incorporated into the electron transport problem through a boundary condition (the spin-scattering self-energy).

In Sec II, coupling between the number of available electrons/holes ( $[G^n]/[G^p]$ ) at a state and the in/out-flow ( $[\Sigma_S^{in}]/[\Sigma_S^{out}]$ ) to/from that state is related through the fourth order scattering tensor  $[D^n]/[D^p]$  in Eq. (8). These in/out-scattering matrices described within the NEGF model have to be calculated self-consistently through the correlation and spectral functions. A general self-consistent solution scheme for the NEGF model considered here is discussed in Sec II.

For elastic ( $\hbar\omega = 0$ ) and point like ( $\delta(r - r')$ ) spin exchange scattering processes considered here, tensor relationship given in Eq. (8) simplifies to:

$$\Sigma_{S;\sigma_i\sigma_j}^{in,out} = D_{\sigma_i\sigma_j;\sigma_k\sigma_l}^{n,p} \times G_{\sigma_k\sigma_l}^{m,p}. \quad (16)$$

The spin exchange scattering tensors  $[D^n]/[D^p]$  can be calculated from the spin scattering hamiltonian. A wavefunction based derivation is presented for *isotropic* and *point like* electron-impurity spin exchange interactions in the Appendix for an interaction Hamiltonian of type  $H^{int} = J\vec{\sigma} \cdot \vec{S}$ .

Accordingly,  $[D^n]/[D^p]$  scattering tensors relate the electron/hole  $[G^n]/[G^p]$  correlation matrices with the (2x2) block diagonal elements of  $[\Sigma_S^{in}]/[\Sigma_S^{out}]$  inscattering/outscattering matrices of form;

$$\Sigma_S^{in,out} = \begin{pmatrix} \left(\bar{\Sigma}_S^{in,out}\right)_{1,1} & \bar{0} & \dots & \bar{0} \\ \bar{0} & \left(\bar{\Sigma}_S^{in,out}\right)_{2,2} & \dots & \bar{0} \\ \vdots & \vdots & \ddots & \vdots \\ \bar{0} & \bar{0} & \dots & \left(\bar{\Sigma}_S^{in,out}\right)_{N,N} \end{pmatrix} \quad (17)$$

through the tensor relationship (*shown below in matrix*

*format*) for the corresponding lattice sites "jj" with mag-

netic impurities;

$$\left\{ \begin{array}{l} \left( \sum_{S,\uparrow}^{in,out} \right)_{jj} \\ \left( \sum_{S,\downarrow}^{in,out} \right)_{jj} \\ \left( \sum_{S,\uparrow}^{in,out} \right)_{jj} \\ \left( \sum_{S,\downarrow}^{in,out} \right)_{jj} \end{array} \right\} = J^2 N_I \overbrace{\begin{bmatrix} 0 & F_u & 0 & 0 \\ F_d & 0 & 0 & 0 \\ 0 & 0 & 0 & 0 \\ 0 & 0 & 0 & 0 \end{bmatrix}}^{[D^{n,p}]} \left\{ \begin{array}{l} \left( G_{\uparrow\uparrow}^{n,p} \right)_{jj} \\ \left( G_{\downarrow\downarrow}^{n,p} \right)_{jj} \\ \left( G_{\uparrow\downarrow}^{n,p} \right)_{jj} \\ \left( G_{\downarrow\uparrow}^{n,p} \right)_{jj} \end{array} \right\} \quad (18)$$

where  $N_I$  is the number of magnetic impurities and  $F_u/F_d$  represents fractions of spin-up/spin-down impurities for an uncorrelated ensemble ( $F_u + F_d = 1$ ).

This complex looking tensor relationship can be understood heuristically from elementary arguments. Simply, the in/out-scattering into *spin-up* component is proportional to the density of the *spin-down electrons/holes* times the number of *spin-up impurities*,  $N_I F_u$ :

$$\left( \sum_{S,\uparrow}^{in,out} \right)_{jj} = J^2 N_I F_u \left( G_{\downarrow\downarrow}^{n,p} \right)_{jj}. \quad (19)$$

Similarly, the in/out-scattering into *spin-down* component is proportional to the density of the *spin-up electrons/holes* times the number of *spin-down impurities*,  $N_I F_d$ :

$$\left( \sum_{S,\downarrow}^{in,out} \right)_{jj} = J^2 N_I F_d \left( G_{\uparrow\uparrow}^{n,p} \right)_{jj}. \quad (20)$$

### C. Incoherent Regime: Results

*Incoherent* tunneling regime device characteristics in the presence of magnetic impurities are studied for a fixed barrier height  $U_{barr} = 1.6$  eV [Fig. 3 (c)] with changing barrier thicknesses and electron-impurity spin exchange interactions ( $J^2 N_I = 0 - 6$  eV). *Nonlinear* decay of *JMRs* at all barrier thicknesses is observed with increasing spin-exchange interactions due to the mixing of independent spin-channels [5, 6] while the *normalized JMRs* are proven to be thickness independent (*inset*). This observation is attributed to the elastic nature of the spin exchange interactions yielding a total drop in *JMR* ( $E_z$ ) values at all  $E_z$  energies in Eq. (15) while preserving the *normalized*  $\omega(E_z)$  carrier distributions [Fig. 3(d)].

Further analysis demonstrates that exchange interaction scattering processes are suppressed with increasing tunneling barrier heights [Fig. 4(a)] leading to improvements in *JMR* values in addition to the coherent effects [Fig. 3(a)]. This observation is in agreement with previous studies [7, 8]. Another interesting feature is that *normalized JMRs* can be mapped into a *single universal curve* using a tunneling barrier height dependent scaling constant  $c(U_{barr})$ .

This allows us to choose a particular value of barrier height [ $U_{barr} = 1.6$  eV] and adjust a *single parameter*  $J$  to fit our NEGF calculations [Fig. 4(c-d)] with experimental measurements obtained from  $\delta$ -doped MTJs

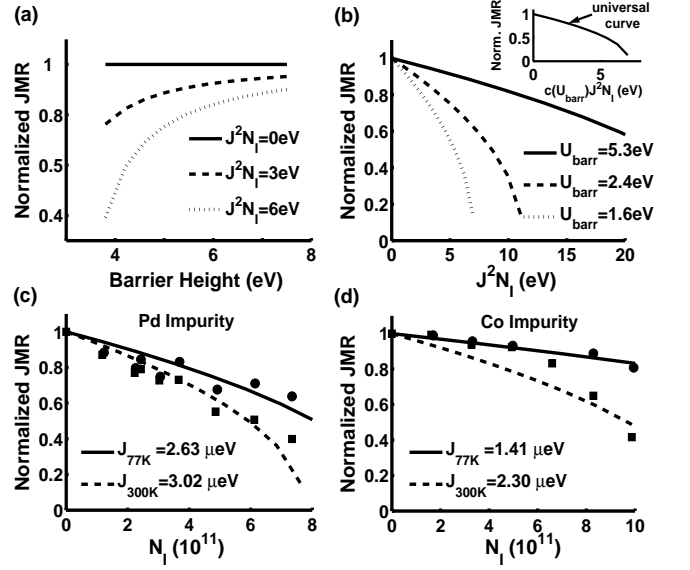


FIG. 4: (a) Elastic spin-flip scattering processes are shown to be suppressed with increasing tunneling barrier heights. (b) *Normalized JMRs* for different tunneling barrier heights and varying spin-exchange couplings can be scaled into a *single universal curve* (inset). Experimental data taken at 77K and 300K is compared with theoretical analysis in the presence of (c) palladium and (d) cobalt magnetic impurities with increasing impurity concentrations.

[5]. Submonolayer impurity thicknesses given in the measurements are converted into number of impurities using material concentrations of Pd/Co impurities and device cross sections ( $6 \times 10^{-4}$  cm<sup>2</sup>) [5].

*Close fitting* to the experimental data are observed at 77K [Fig. 4(c-d)] using physically reasonable exchange coupling constants of  $J = 2.63\mu\text{eV}/1.41\mu\text{eV}$  for devices with Pd/Co impurities [24]. However, experimentally observed temperature dependence of *normalized JMR* ratios can not be accounted for by our model calculations. Broadenings of the electrode Fermi distributions due to changing temperatures from 77K to 300K seem to yield variations in *normalized JMR* ratios within a linewidth. As a result, different  $J$  exchange couplings are used in order to match the experimental data taken at 300K.

For *Pd doped* MTJs, a relatively small variation in  $J$  exchange couplings is needed ( $J_{300}/J_{77} = 1.16$ ) in order to match the experimental data at 300K. This small temperature dependence could be due to the presence of some secondary mechanisms not included in our calculations. One possible explanation includes the presence of impurity-assisted conductance contribution through the defects (*possibly created by the inclusion of magnetic impurities within the barrier*) which is known to be strongly temperature dependent [25]. In fact, the contribution of the impurity-assisted conductance is proportional with the impurity concentrations in accordance with the experimental measurements [Fig. 4(c)].

On the contrary, for *Co doped* MTJs, there's a clear

distinction for *normalized JMR* ratios at different temperatures [Fig. 4(d)] which can not be justified by the presence of secondary mechanisms. Fitting these large deviations require large variations in  $J$  exchange coupling parameters [ $J_{300}/J_{77} = 1.73$ ] and we propose this to be a result of thermally driven *low-spin/high-spin phase* transition [26, 27], since the oxidation state of the cobalt atoms could be in  $\text{Co}^{+2}$  ( $S = 3/2$ , high-spin) or  $\text{Co}^{+3}$  ( $S = 0$ , low-spin) state or partially in both of the states depending on the oxidation environment. Such thermally driven low-spin/high-spin phase transitions for metal-oxides is predicted by theoretical calculations and observed in previous experimental studies [26, 27], although it is not discussed in connection with MTJs community.

#### IV. SUMMARY

*Summary:* A quantum transport model incorporating spin-flip scattering processes is presented using the NEGF formalism within the self-consistent Born approximation. Spin-flip scattering and quantum effects are simultaneously captured. Spin scattering operators are derived for the specific case of electron-impurity spin-exchange interactions and the formalism is applied to spin dependent electron transport in MTJs with magnetic impurity layers. The theory is benchmarked against

experimental data involving both coherent and incoherent transport regimes. *JMRs* are shown to decrease both with barrier thickness and with spin-flip scattering but our unified treatment clearly brings out the difference in the underlying physics [Fig. 3]. The deteriorating effect of the magnetic impurities on *JMR* ratios diminishes with increasing tunneling barrier heights [Fig. 4(a)]. Our numerical results show that both barrier height and the exchange interaction constant  $J$  can be subsumed into a single parameter that can explain a variety of experiments [Fig. 4]. Interesting differences between devices having Pd and Co impurities are pointed out, which could be signatures of low-spin/high-spin phase transitions in cobalt oxides. Small differences in spin-states/concentrations of magnetic impurities are shown to cause large deviations in *JMRs*.

#### Acknowledgments

This work was supported by the MARCO focus center for Materials, Structure and Devices and the NSF Network for Computational Nanotechnology. Part of this work was carried out at the Jet Propulsion Laboratory under a contract with the National Aeronautics and Space Administration NASA funded by ARDA.

- 
- [1] R. Landauer, *Physica Scripta* **T42**, 110 (1992).
  - [2] Y. Li and C. Chang, *Phys. Lett. A* **287**, 415 (2001).
  - [3] C. C. Y. Li and Y. Yao, *J. Appl. Phys.* **91**, 8807 (2002).
  - [4] D. X. L. Sheng and D. N. Sheng, *Phys. Rev. B* **69**, 132414 (2004).
  - [5] R. Jansen and J. Moodera, *J. of Appl. Phys.* **83**, 6682 (1998).
  - [6] R. Jansen and J. Moodera, *Phys. Rev. B* **61**, 9047 (1998).
  - [7] A. Davis, Ph.D. thesis, Tulane University (1994).
  - [8] J. M. A.H. Davis, *J. Phys.: Condens. Matter* **14**, 4365 (2002).
  - [9] S. Datta, *Quantum Transport: Atom to Transistor* (Cambridge University Press, Cambridge, 2005).
  - [10] M. Stearns, *J. Magn. Magn. Mater.* **5**, 167 (1977).
  - [11] T. M. K. Matsuda, A. Kamijo and H. Tsuge, *J. of Appl. Phys.* **85**, 5261 (1999).
  - [12] G. N. J. L. H. S. S. Y. Z. H. Chen, Q. Y. Xu and Y. W. Du, *J. of Appl. Phys.* **85**, 5798 (1999).
  - [13] J. Zhang and R. M. White, *J. of Appl. Phys.* **83**, 6512 (1998).
  - [14] A. K. T. Mitsuzuka, K. Matsuda and H. Tsuge, *J. of Appl. Phys.* **85**, 5807 (1998).
  - [15] R. C. W. Oepts, H. J. Verhagen and W. J. M. de Jonge, *J. of Appl. Phys.* **86**, 3863 (1999).
  - [16] J. D. B. A. E. R. S. Beech, J. Anderson and D. Wang, *IEEE Trans. Mag.* **32**, 4713 (1996).
  - [17] K. T. H. F. H. Yamanaka, K. Saito, *IEEE Trans. Mag.* **35**, 2883 (1999).
  - [18] J. N. J.S. Moodera and R. van de Veerdonk, *Phys. Rev. Lett.* **80**, 2941 (1998).
  - [19] J. Sun and P. Freitas, *J. of Appl. Phys.* **85**, 5264 (1999).
  - [20] R. J. C.H. Shang, J. Nowak and J. Moodera, *Phys. Rev. B* **58**, 2917 (1998).
  - [21] J. Moodera and L. Kinder, *Phys. Rev. Lett.* **74**, 3273 (1995).
  - [22] V. Henrich and P. Cox, *The Surface Science of Metal Oxides* (Cambridge University Press, Cambridge, 1994).
  - [23] J. Simmons, *J. Appl. Phys.* **34**, 1793 (1963).
  - [24] B. Kane, *Nature* **393**, 133 (1998).
  - [25] R. S. et al., *J. of Appl. Phys.* **85**, 5258 (1999).
  - [26] T. Kambara, *J. Chem. Phys.* **70**, 4199 (1979).
  - [27] S. Biernacki and B. Clerjaud, *Phys. Rev. B* **72**, 024406 (2005).